UNIVERSITY OF BIRMINGHAM

University of Birmingham
Research at Birmingham

# Different bed configurations and time ratios: Performance analysis of low-grade heat driven adsorption system for cooling and electricity

Al-Mousawi, Fadhel; Al-Dadah, Raya; Mahmoud, Saad

**Publisher Rights Statement:**
Checked for eligibility: 03/07/2017

1  **Different bed configurations and time ratios: Performance analysis of low-grade heat**
2  **driven adsorption system for cooling and electricity**

3

4  Fadhel Noraldeen Al-Mousawi[a,b*], Raya Al-Dadah[a], Saad Mahmoud[a]

5  [a] Department of Mechanical Engineering, University of Birmingham, B15 2TT, United Kingdom

6  [b] Department of Mechanical Engineering, University of Karbala, Karbala, Iraq

7  [*] e-mail address: fna397@bham.ac.uk (fadhelnor@gmail.com)

8

## 9  Abstract

10  In this study, different multi-bed water adsorption systems have been used to generate cooling and

11  electricity at the same time using 9 different cases including 7 bed configurations and 7 time ratios (R =

12  total switching and adsorption time /the total switching and desorption time) utilizing advanced

13  adsorption materials such as AQSOA-Z02 and MOF Aluminium-Fumarate additionally to traditional

14  Silica-gel. A MATLAB Simulink program of multi-bed adsorption system for cooling and power

15  generation has been developed to investigate the effect of using different cases on the overall system

16  performance. Results showed that using three-bed configuration with time ratio of (R=1/2) produced the

17  highest specific cooling power (SCP) and specific power (SP) for Silica-gel (for all heat source

18  temperature range), Aluminium-Fumarate (for heat source temperature higher than 120 °C) and AQSOA-

19  Z02 (at heat source temperature of 160 °C). Moreover, using two-bed configuration with time ratio of

20  (R=1) generates the highest coefficient of performance (COP) for all adsorption materials within the

21  range of heat source temperature used in this study. Results also, showed that maximum COP of 0.64 can

22  be achieved using Silica-gel, while maximum SCP, SP and adsorption power efficiency of 650 W/kg$_{ads}$,

23  64 W/kg$_{ads}$, 4.6 % can be achieved using AQSOA-Z02.

24  Keywords: Multi-bed, Time Ratio, Adsorption, Cooling and Electricity, AQSOA-Z02, Aluminium-
25  Fumarate, Silica-gel

## 26  1.  Introduction

27  Nowadays, searching for alternative energy sources becomes an essential aim because of the large energy

28  consumption around the world, while electricity is still mainly generated by burning fossil fuel which

29  rises $CO_2$ emissions. In hot countries, refrigeration and air conditioning equipment used in houses and

30  offices consume a large amount of electricity, while millions of people, especially in poor countries still

31  face difficulties to access low-cost and reliable energy sources. Adsorption technology offers the potential

32  of using low-grade heat sources such as solar, geothermal and waste heat from industrial processes to

33  produce cooling and electricity simultaneously. Fossil fuel is still the main source of energy since

34  decades; however, the abundant renewable resources such as low-grade heat from solar energy or waste

heat from industrial processes can be converted into useful cooling and electricity using promising clean energy technologies like absorption, adsorption and Organic Rankine cycle (ORC). Such renewable technologies can be improved to face the serious concerns of the global warming around the world and reduce the emissions of the $CO_2$. A number of researchers investigated the absorption cooling technology experimentally [1] and numerically [2], while many researchers investigated means of improving the adsorption cooling technology using multi-bed [3], multi-stages [4], utilizing a number of working pairs [5] through modelling [6] and experimental work [7]. Gonzalez-Gil et al [8] experimentally studied a solar air-conditioning water/lithium bromide absorption system and reported a COP of about 0.6 with a cooling capacity between 2 and 3.8 kW. Wang [9] used new ideas to integrate heat pipes with adsorption water chiller achieving average cooling and COP of 10 kW and 0.4 using heat source temperature of 85 °C. Gong et al [10] examined experimentally the cooling effect of lithium chloride and Silica-gel composite adsorption chiller with methanol. Results showed that, compared to the Silica-gel/water unit, the SCP and COP of the composite were increased by 16.3% and 24.2%.

Generating power (electricity) at high efficiency using low-grade heat sources like solar energy, geothermal energy and waste heat from industrial processes is still a strategic goal for many researchers. Kalina cycle and Organic Rankine cycle (ORC) have the capability of generating electricity using such low-grade heat sources [11, 12]. Le et al. [13] investigated a number of ORC fluids to optimize the performance of basic and regenerative supercritical ORC utilizing heat source temperature of 150 °C. Results showed that the maximum efficiencies of the basic and regenerative were 11.6 % and 13.1 % respectively using R152a, while the maximum power generated was 4.1 kW using R1234ze.

In order to achieve both cooling and electricity at the same time, a number of researchers designed and investigated combined systems for cooling and electricity utilizing low-grade heat sources. Vijayaraghavan and Goswami [14] studied two configurations to combine an absorber and a turbine in one system to generate cooling and electricity. Results showed that efficiency can be enhanced by up to 25%, while exergy analysis showed that RUE (resource utilization efficiency) can be improved. Liu and Zhang [15] have proposed a cogeneration system consisting of ammonia/water Rankine cycle and an ammonia absorption refrigeration cycle utilizing heat source temperature of around 450 °C to generate cooling and power simultaneously. Results showed that maximum exergy efficiency of 58% can be

63 achieved and the energy consumption can be reduced by 18.2% compared to conventional separate

64 systems. Zheng et al. [16] have suggested a combined absorption cooling and power system based on

65 Kalina cycle's principles. The cycle produced cooling and power at the same time with an overall thermal

66 and exergy efficiencies of 24.2% and 37.3% respectively. Zhang and Lior [17] investigated an

67 ammonia/water cogeneration system to produce cooling and power at the same time. The system works in

68 parallel mode with an ammonia/water Rankine cycle and an ammonia refrigeration cycle. Energy and

69 exergy efficiencies were assessed and they had the values of 27.7% and 55.7%, respectively using heat

70 source temperature of 450 °C. Absorption technology can generate cooling and electricity simultaneously,

71 however, such systems have large size, besides ammonia is a toxic material which may cause serious

72 health risks. On the other hand, adsorption technology has robust construction, ease of installation, and in

73 many cases, is considered to be more advantageous than absorption systems. In addition, There are no

74 opportunities of crystallization, corrosion, risky leaks and the power consumption is negligible [18].

75 Adsorption is promising technology that recently used to generate cooling and electricity at the same time

76 utilizing low-grade heat sources. This technology has a number of advantages like very few moving parts,

77 high reliability, capability over a wide range of heat source temperatures with appropriate adsorption

78 materials, and environmentally friendly refrigerants [19]. Jiang et al. [20] have introduced a resorption

79 cogeneration system to generate cooling and power simultaneously. Results showed that with using heat

80 recovery the cycle can achieve electrical efficiency and COP of 9.5–15.8% and 0.416–0.691 respectively.

81 Wang et al. [21] have presented a novel resorption cogeneration cycle for cooling and electricity

82 simultaneously based on ammonia adsorption cooling technology. Results showed that utilizing a driving

83 temperature higher than 100 $^\circ$C can produce a maximum overall exergy efficiency of 0. 9 and a COP of

84 0.77. Bao et al. [22] have studied an adsorption cogeneration prototype to generate power and cooling

85 simultaneously. The COP and the exergy efficiency of the cycle are 0.57 and 0.62 respectively.  Bao et al.

86 [23] built chemisorption cogeneration prototype using calcium chloride and activated carbon was to

87 generate power and cooling simultaneously. Results showed that the system could achieve a minimum

88 value of 5.4 °C at the evaporator and it could produce 490 W of power. L. Jiong et al. [24] have designed

89 and studied a resorption cogeneration cycle for cooling and power using a scroll expander with $MnCl_2$-

90 $CaCl_2$-$NH_3$. Results showed that maximum power of 300W and cooling of 2kW as well as 91 min of cold

3

storage function can be achieved. Yiji Lu et al [25] improved the ammonia resorption cogeneration cycle proposed by Wang et al with mass and heat recovery using twelve different working pairs. Results showed that COP increased by 38% and 35% utilizing $NiCl_2$ and $MnCl_2$ respectively. The efficiency of electricity has also been improved from 8% to 12% and the second law efficiency reached 41% using $BaCl_2$–$MnCl_2$. Al- Mousawi et al. [26] simulated a two-bed adsorption system to generate cooling and power simultaneously using AQSOA-Z02/water, MIL101Cr/water and Silica-gel/water using heat source temperature between 80 and 160 °C. Results showed that, the system can generate SP of 73 $W/kg_{ads}$, and SCP of 681 $W/kg_{ads}$ (using AQSOA-Z02) and maximum efficiency of 67%. Al-Mousawi el al. [27] designed and modelled a small scale radial inflow turbine with efficiency of 82% to generate electricity of 785 W in addition to cooling from a two-bed adsorption system utilizing AQSOA-Z02/water using heat source temperature of 160 °C. Al-Mousawi et al. [28] studied integrated adsorption-ORC system to simultaneously generate cooling and electricity. Results showed that system can achieve efficiency, SP and SCP of 70%, 208 $W/kg_{ads}$ and 616 $W/kg_{ads}$ respectively.

In adsorption cooling systems, as the cycle time increases the coefficient of performance increases, and this decreases the specific cooling power (SCP) [29]. Many researchers have studied the performance optimisation of two-bed adsorption cooling systems [29, 30] and three-bed adsorption cycles [31]. Glaznev and Aristov [32] found experimentally that desorption process is faster than adsorption process by 2.2 to 3.5. Sapienza et al. [33] experimentally found that the best performance can be achieved with the adsorption time is 7 times longer than desorption timer using driving temperature of 90 °C. Zajaczkowski [34] found that in a three-bed adsorption system and for switching time 30 s and adsorption time 300 s, the desorption/adsorption time ratio is almost 0.6 gives the highest improvement in SCP and COP. Graf et al. [35] showed that the adsorption and desorption times can affect the COP and SCP and they found that the maximum values of COP and SCP are 268 W/kg and 0.51 respectively using adsorption time of 200 s and desorption time of 125 s.

None of the previous work studied the effect of using different bed configurations and bed arrangement either in series or in parallel besides the effect of adsorption/desorption time ratio on the overall performance of the adsorption system for cooling and electricity. In this paper, 9 different cases including 7 different configurations and 7 time ratios have been investigated. Different cases are

compared to the two-bed adsorption system for cooling and electricity in terms of system coefficient of performance (COP), specific cooling power (SCP), specific power generated (SP) and adsorption power efficiency. In addition, advanced adsorption pairs of AQSOA-ZO2/water and Aluminium-Fumarate MOF/water have been investigated and compared to Silica-gel/water, while environmentally friendly fluid of water has been used as adsorption working fluid.

## 2. Two-bed adsorption system for cooling and electricity

Figure 1(a) shows a schematic diagram of a basic cooling adsorption system (BCAS) which contains two adsorption beds, condenser, and evaporator. Adsorption is an exothermic process, as a result cooling is needed to cool the adsorber (cold bed) during the adsorption process using cooling source CS in order to adsorb the refrigerant from the evaporator and produce the cooling capacity. Desorption is an endothermic process, so heating is needed during the desorption process to release the refrigerant (water vapour) from the desorber (hot bed) using heating source HS like solar energy or waste heat. Subsequently, condenser cools the hot refrigerant coming from the desorber to feed the evaporator with liquid refrigerant that needed to produce cooling continuously.

Figure 1(b) shows a schematic diagram of the adsorption system for cooling and electricity as described by a number of literature [22, 26, 27, 36] which consisting of adsorber, desorber, condenser, evaporator and expander (turbine) located between the hot bed (desorber) and the condenser to extract the kinetics energy from the refrigerant vapour at high temperature and pressure. Figure 2(a) shows the P-T diagram of BCAS, process 1-2 is isoteric heating (preheating switching), processes (2-3'/2-3) are isobaric desorption/condensation, process 3'-4' is isoteric cooling (precooling switching) and finally processes (4'-1/4-1) are isobaric adsorption/evaporation. Figure 2(b) shows the P-T diagram of the adsorption system for cooling and electricity and in this system, the pressure of the condenser have to be lower than the pressure of the hot bed to make the pressure difference required to generate power (electricity) in the expander (turbine). Process 1-2 is isoteric heating same as in BCAS, while process 2-3 is expansion process from the bed pressure (maximum pressure) to the condenser pressure, process 3-4 is isobaric condensation while the rest processes are similar to BCAS.
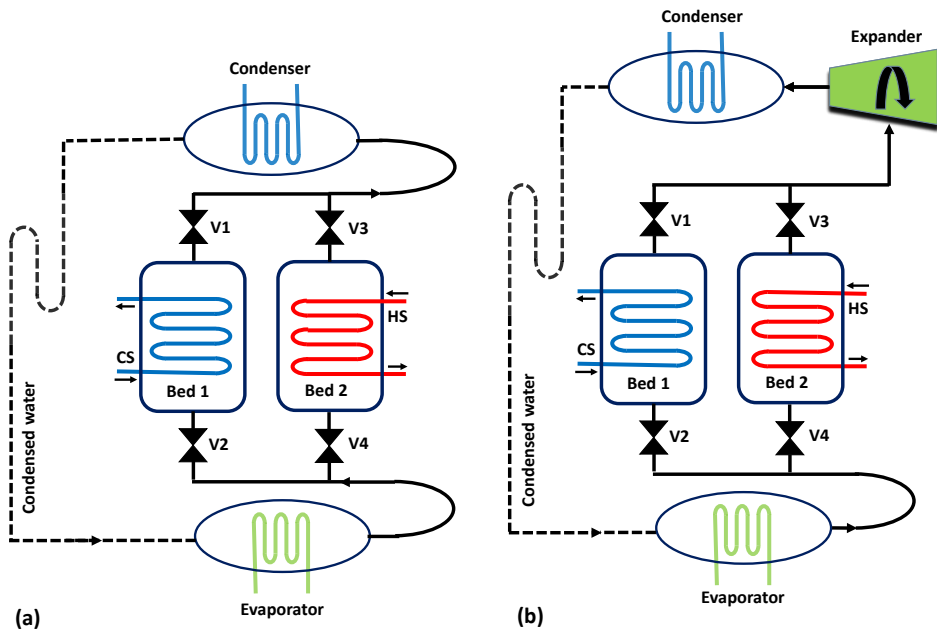
**Figure 1: Schematic diagram of (a) Basic cooling adsorption system (BCAS) (b) Adsorption system for cooling and electricity.**
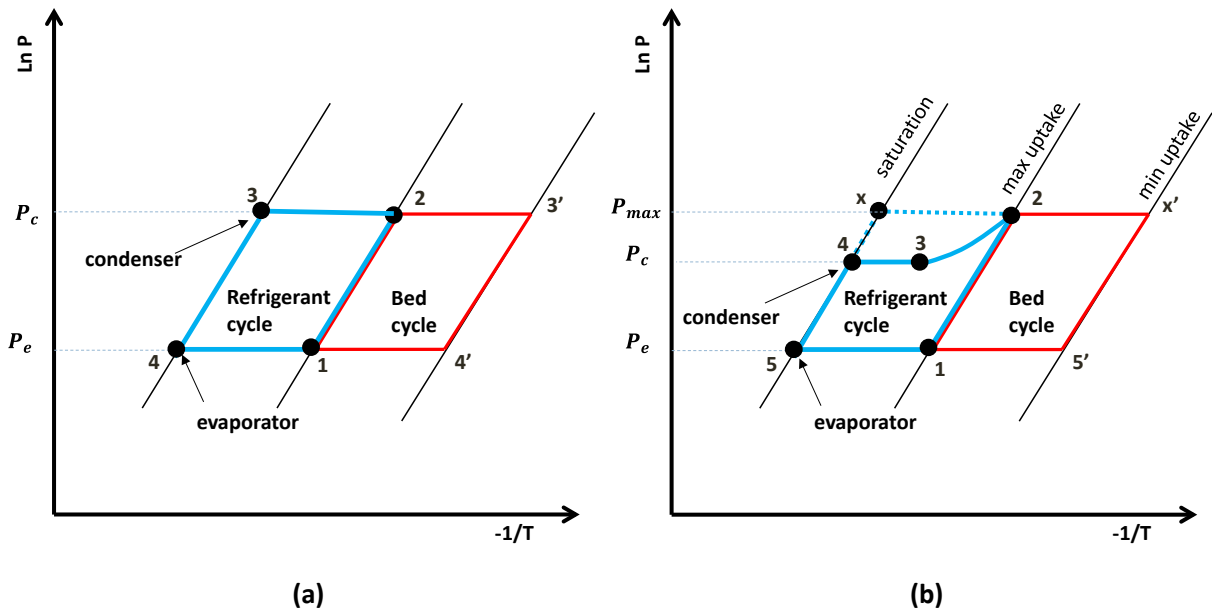


**Figure 2: P-T diagram (a) Basic cooling adsorption system (BCAS) (b) Adsorption system for cooling and electricity.**

## 3. Multi-bed adsorption system for cooling and electricity

Multi-bed adsorption system for cooling and electricity has the same principle of work for the two-bed adsorption system for cooling and electricity as discussed in section 2. Instead of using only two adsorption beds, a number of adsorption beds are used in the same system. Usually when two-bed is used in the adsorption system the total adsorption time (adsorption time +switching time) is equal to the total

156 desorption time (desorption time +switching time) .i.e. the time ratio R=1. This study aims to investigate

157 the effect of using multi-bed configurations with a number of time ratios (R) on the overall system

158 performance. For example, in the three-bed adsorption system with R=1/2 shown in Figure 3 (a), bed 1

159 starts with desorption phase (20s switching time + 140s net desorption) as shown in Figure 4 with zero

160 delay time, then it switches to adsorption phase (20s switching time + 300s net adsorption). Bed 2 and

161 bed 3 work in similar way as shown in Figure 4, but with delay times of 160s and 320s respectively. The

162 same concept can be used for the four, five and six-beds systems as shown in Figure 3 (b), (c) and (d)

163 with R of 1/3, 1/4 and 1/5 respectively.

164 Besides two (2B), three (3B), four (4B), five (5B) and six-bed (6B) systems another two configurations

165 are investigated in this study. The first one is the four-bed system which consisting of a pair of two beds

166 working in parallel with R=1 as shown in Figure 3(e), while the other one is six-bed which consisting of a

167 pair of three beds working in parallel with R=1/2 as shown in Figure 3(f). Thus in this work, 9 different

168 cases including 7 different bed configurations and 7 adsorption/desorption ratios are investigated to find

169 the best configuration and adsorption/desorption ratio in terms of performance, specific cooling and

170 specific power output.



171

7

**(c)**

172



**(d)**

173

174

**(e)** Evaporator

**(f)** Evaporator
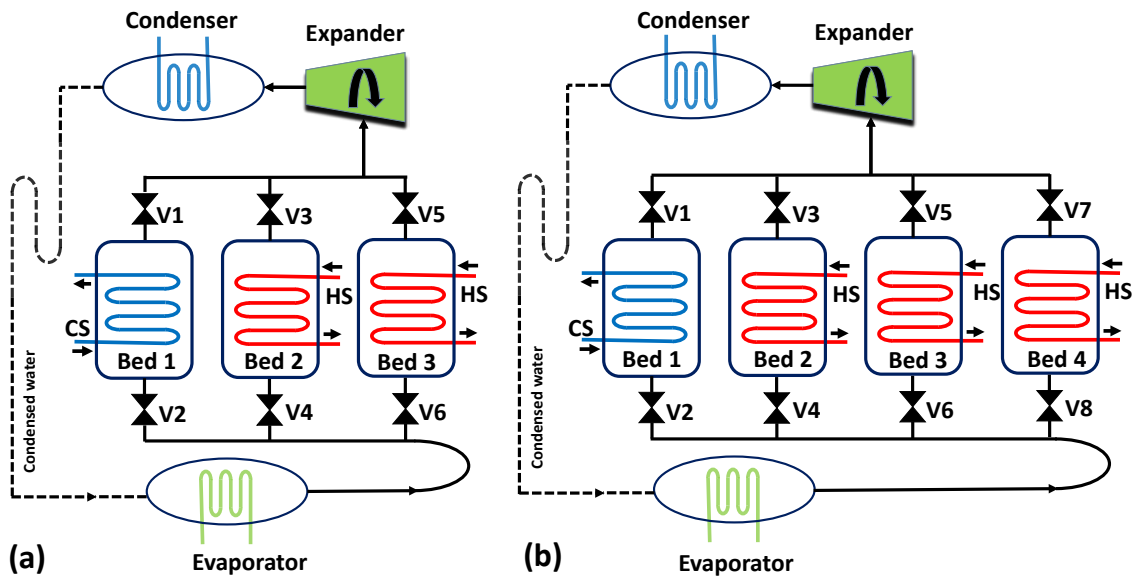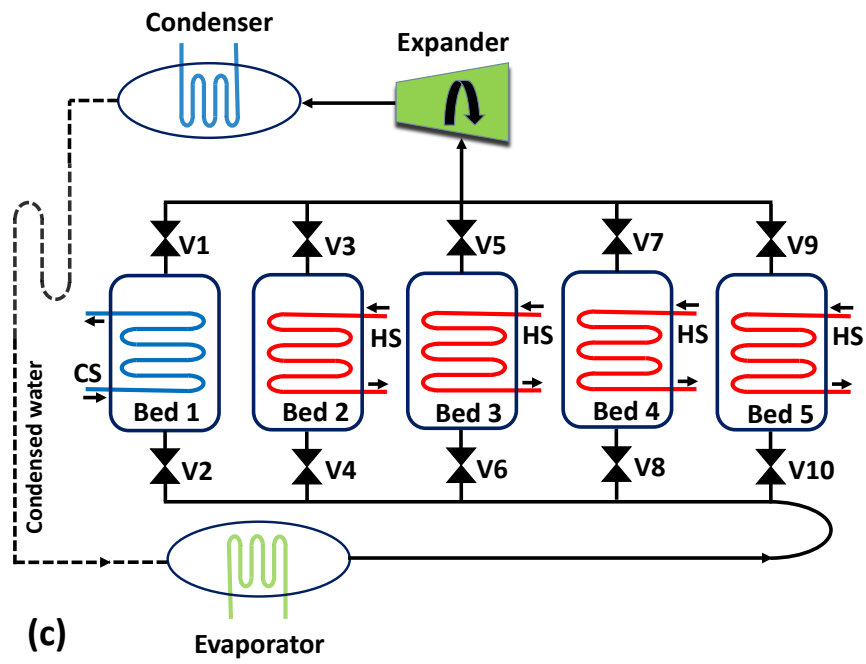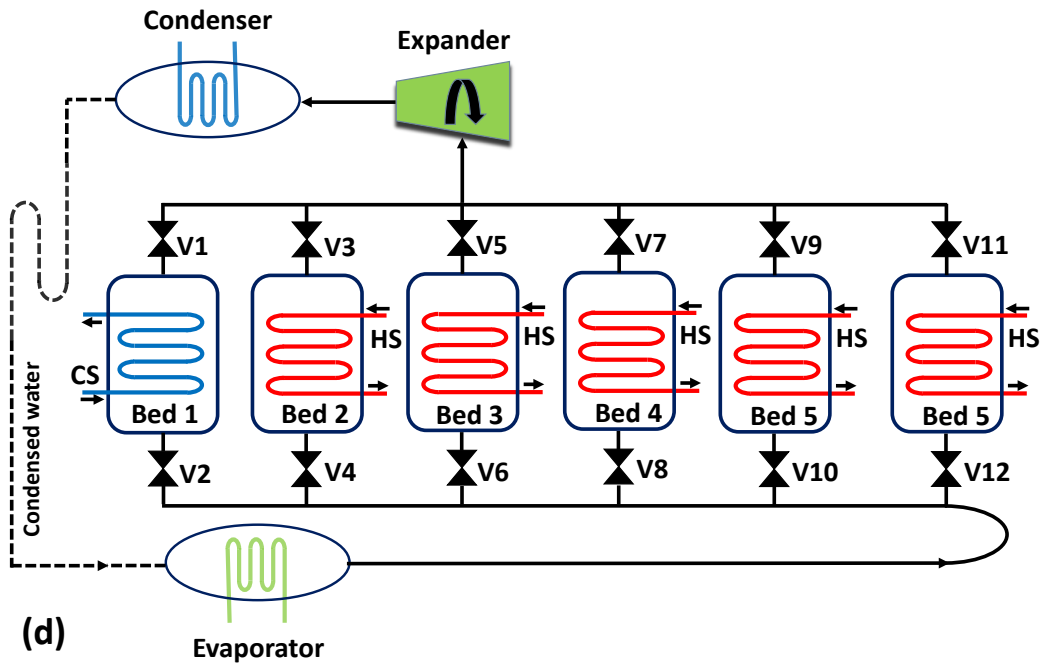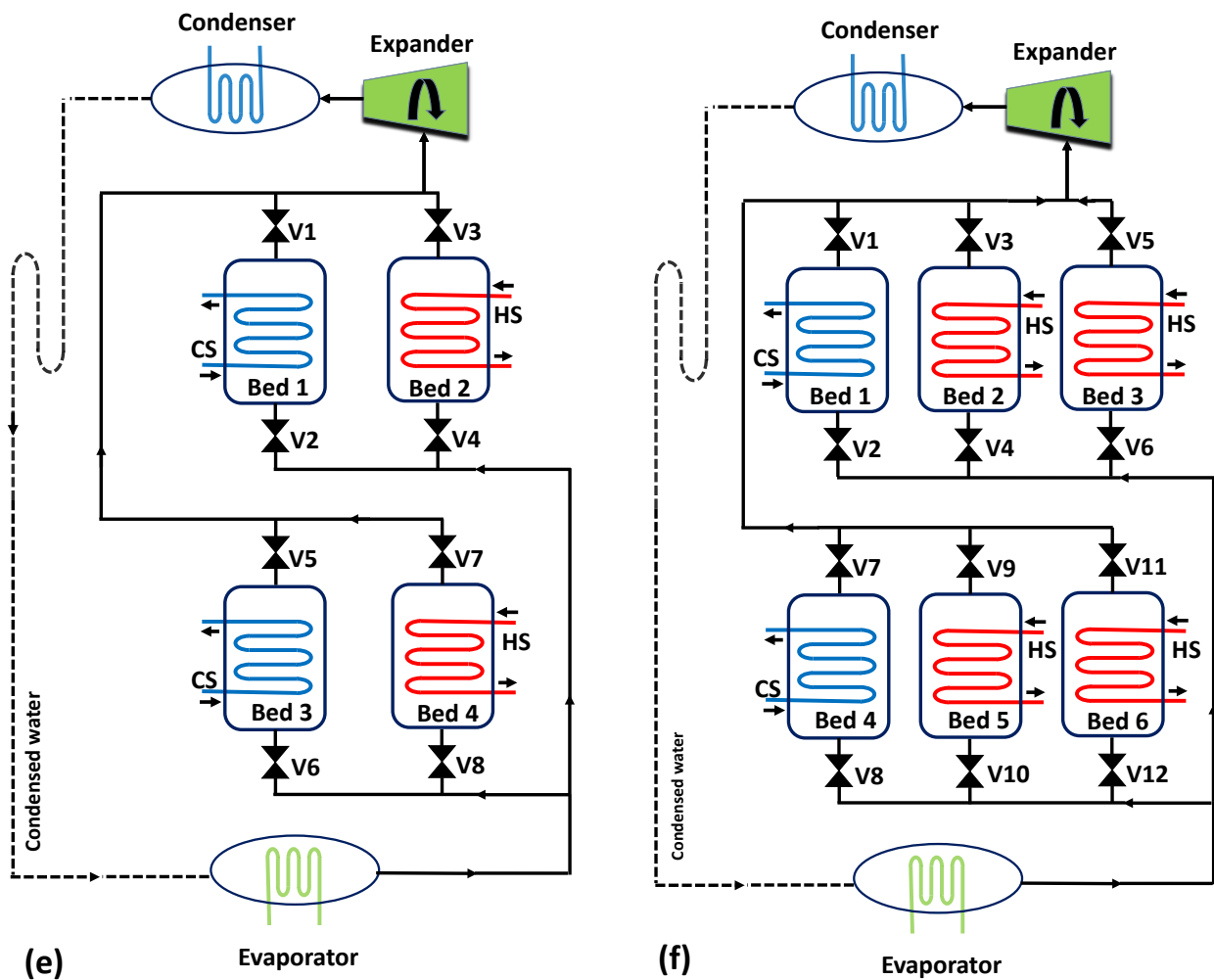
Figure 3: Schematic diagram of multi bed adsorption system for cooling and electricity (a) three-bed (b) four-bed in series (c) five-bed (d) six-bed in series (e) four-bed in parallel and (f) six-bed in parallel.
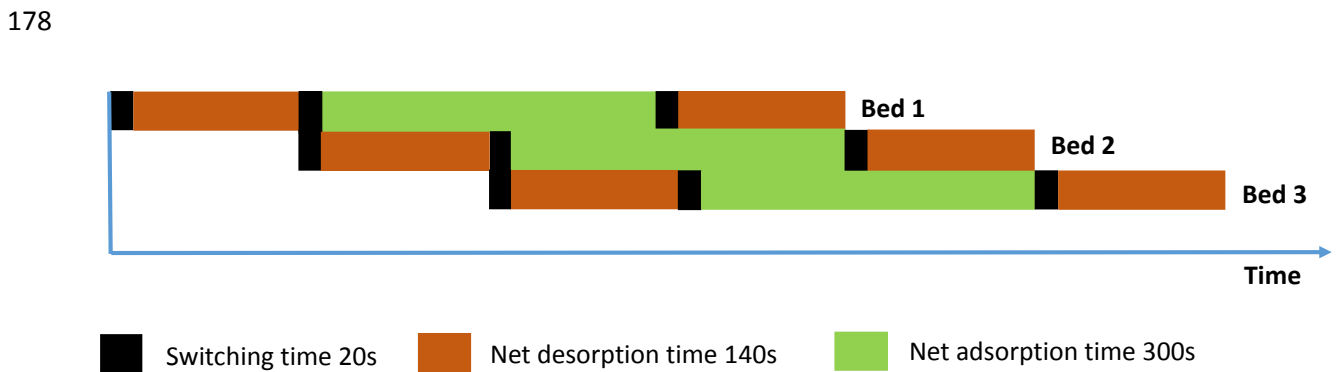


Switching time 20s    Net desorption time 140s    Net adsorption time 300s

Figure 4: Time allocation of the three-bed adsorption system for cooling and electricity with R=1/2.

## 4. Mathematical Modelling

In this study, new advanced adsorption pairs of AQSOA-Z02/water and Aluminium-Fumarate/water are used and compared to Silica-gel/water. The adsorption equilibrium for AQSOA-ZO2/water can be written as [37]

$$x_{eq} = x_o \left[ \frac{k(\frac{P_s(T_w)}{P_s(T_a)})^n}{1+(k-1)(\frac{P_s(T_w)}{P_s(T_a)})^n} \right] \tag{1}$$

$$\text{k} = \alpha exp\left[ n(Q_{st} - h_{fg})/(RT^{bed}) \right] \tag{2}$$

Where, $P_s(T_w)$ and $P_s(T_a)$ are the saturation vapour pressure at water vapour temperature and adsorbent temperature respectively and the constants $x_o$, $\alpha$, n and $Q_{st}$ are taken from [26].

For Aluminium-Fumarate/water, the adsorption equilibrium of equation (3) is obtained from [38] and listed in Table 1.

$$x_{eq} = f(A) \tag{3}$$

*Where*

$$A = -RT^{bed} ln(\frac{P_s(T_w)}{P_s(T_a)}) \tag{4}$$

**Table 1: Aluminium-Fumarate/water isotherms of Eq. (3)**

| | |
|---|---|
| *A< 2900* | $x_{eq} = 0.5948 - 3.12\text{E-}4A + 1.68302\text{E-}7A^2 - 3.124455\text{E-}11A^3$ |
| *A> 3987* | $x_{eq} = 0.111993 EXP(-0.000258797A)$ |
| *2900≤A≤3987* | $x_{eq} = 2.36129 - 9.93768\text{E-}4A + 1.05709\text{E-}7A^2$ |

For Silica-gel/water, the modified Freundlich equation is used to present the adsorption equilibrium [39-41] as:

$$x_{eq} = A(T_s) \left[ \frac{P_s(T_w)}{P_s(T_a)} \right]^{B(T_s)} \tag{5}$$

where

$$A(T_s) = A_o + A_1 T_s + A_2 T_s^2 + A_3 T_s^3 \tag{6}$$

$$B(T_s) = B_o + B_1 T_s + B_2 T_s^2 + B_3 T_s^3 \tag{7}$$

The constants of equations (6) and (7) are obtained from [41, 42].

Linear driving force (LDF) equation is used to describe the adsorption/desorption rate as [39, 40, 43]

$$\frac{dx}{dt} = k_o exp\left( -\frac{E_a}{RT} \right)(x_{eq} - x) \tag{8}$$

210  The kinetics constants ($k_o$ and $E_a$) of equation (8) are taken from reference [44] for AQSOA-ZO2/water,

211  from reference [38] for Aluminium-Fumarate/water and from references [39, 40] for Silica-gel/water.

212  Lumped model method is used define the energy balance in adsorption beds, where the adsorbent, the

213  adsorbate and the bed materials are assumed to be at the same temperature during the cycle time [43, 45,

214  46].

$$\left(Mc_{p_{eff}}^{bed}\right)\frac{dT^{bed}}{dt} + \left(M_a x_i^{bed} c_p\right)\frac{dT_i^{bed}}{dt} = \varphi M_a \left(\frac{dx_i^{bed}}{dt}\right)(Q_{st}) - \left(\dot{m}c_p\right)_j \left(T_{j,o} - T_{j,in}\right) \qquad (9)$$

215

216  Flag $\varphi$ equals to 0 at switching time and equals to 1 at adsorption/desorption process and the bed outlet

217  temperature is given by [43, 45].

$$T_{j,o} = T_i^{bed} + \left(T_{j,in} - T_i^{bed}\right)\exp\left[\frac{-(UA_r)_i^{bed}}{(\dot{m}c_p)_j}\right] \qquad (10)$$

218

219  The energy balance equations for the condenser can be expressed by [46, 47].

$$\left(Mc_{p_{eff}}^{cond}\right)\frac{dT^{cond}}{dt} = \varphi h_{fg} M_a \frac{dx_{des}^{bed}}{dt} - (\dot{m}c_p)_{cond}\left(T_{w,o} - T_{w,i}\right) - \left(c_p\right)_w \left(T^{bed} - T^{cond}\right)M_a \frac{dx_{des}^{bed}}{dt} \qquad (11)$$

220

221  The condenser outlet temperature is given by [46, 47].

$$T_{w,o} = T^{cond} + \left(T_{w,in} - T^{cond}\right)\exp\left[\frac{-(UA_r)^{cond}}{(\dot{m}c_p)_{cond}}\right] \qquad (12)$$

222

223  The energy balance in the evaporator is expressed as [46, 47].

$$\left(Mc_{p_{eff}}^{evap}\right)\frac{dT^{evap}}{dt} = \varphi h_{fg} M_a \frac{dx_{ads}^{bed}}{dt} - (\dot{m}c_p)_{evap}\left(T_{chill,o} - T_{chill,i}\right) - (c_p)_w \left(T^{cond} - T^{evap}\right)M_a \frac{dx_{des}^{bed}}{dt} \qquad (13)$$

224

225  The outlet temperature of the chilled water can be written as [40, 46, 47].

$$T_{chill,o} = T^{evap} + \left(T_{chill,in} - T^{evap}\right)\exp\left[\frac{-(UA_r)^{evap}}{(\dot{m}c_p)_{evap}}\right] \qquad (14)$$

226

227  The mass balance in the adsorption evaporator can be written as [40, 43, 45, 46].

$$\frac{dM_{ref}}{dt} = -M_a \left[\frac{dx_{des}^{bed}}{dt} + \frac{dx_{ads}^{bed}}{dt}\right] \qquad (15)$$

228

229  Mechanical work produced in the expander (turbine), can be written as below:

230 $$W_{exp} = \frac{\int_0^{t_{cycle}} \eta_{exp}\, \dot{m}_{ads} \Delta h\, dt}{t_{cycle}} \qquad (16)$$

231 Where $\Delta h$ is the enthalpy difference through the adsorption expander and $\dot{m}_{ads}$ is the water mass flow

232 rate through the expander, while $\eta_{exp}$ is the expansion efficiency which is assumed to be ideal for this

233 thermodynamic study. The overall performance of the adsorption system for cooling and electricity can

234 be defined using the terms SCP, SP, COP, adsorption power efficiency ($\eta_{ads}$), COPe and SCPe and written

235 in equations (17-21).

236 $$SCP = \frac{(\dot{m}c_{\text{p}})_{\text{evap}} \int_0^{t_{cycle}} (T_{\text{chill,o}} - T_{\text{chill,i}})\, dt}{M_a t_{cycle}} \qquad (17)$$

237 $$SP = \frac{\int_0^{t_{cycle}} \eta_{exp}\, \dot{m}_{ads} \Delta h\, dt}{M_a t_{cycle}} \qquad (18)$$

238 $$\eta_{ads} = \frac{\int_0^{t_{cycle}} \eta_{exp} \dot{m}_{ads} \Delta h\, dt}{(\dot{m}c_{\text{p}})_{\text{h}} \int_0^{t_{cycle}} (T_{\text{h,o}} - T_{\text{h,i}})\, dt} \qquad (19)$$

239 $$COPe = \frac{(\dot{m}c_{\text{p}})_{\text{evap}} \int_0^{t_{cycle}} (T_{\text{chill,o}} - T_{\text{chill,i}})\, dt + F[\int_0^{t_{cycle}} \eta_{exp}\, \dot{m}_{ads}\, \Delta h\, dt]}{(\dot{m}c_{\text{p}})_{\text{h}} \int_0^{t_{cycle}} (T_{\text{h,o}} - T_{\text{h,i}})\, dt} \qquad (20)$$

240

241 $$SCPe = \frac{(\dot{m}c_{\text{p}})_{\text{evap}} \int_0^{t_{cycle}} (T_{\text{chill,o}} - T_{\text{chill,i}})\, dt + F[\int_0^{t_{cycle}} \dot{m}_{ads} \Delta h\, dt]}{M_a t_{cycle}} \qquad (21)$$

242 The term ($\eta_{ads}$) is used to represent the power generation efficiency of the adsorption system i.e. the ratio

243 of the amount of power generated through the expander (turbine that incorporated within the adsorption

244 system) to the total heat consumed by the adsorption beds. The terms *COPe* (equivalent coefficient of

245 performance) and *SCPe* (equivalent specific cooling power) are used to compare the performance of

246 adsorption system for cooling and electricity to the two-bed basic cooling adsorption system (BCAS). F is

247 the typical COP for compression refrigeration system, which is assumed to be (3) in this work i.e. the

248 power generated, by adsorption system can be converted into cooling again and in order to compare

249 between adsorption system for cooling and electricity system and the basic cooling adsorption system

250 (BCAS).

251 The Exergy efficiency depending on the second law of thermodynamic can be defined as the ratio

252 between the exergy output to the exergy input and it is used to highlight the different grade of cooling and

253 electricity generated by the adsorption system used in this paper. The exergy efficiency can be defined as

254 [17, 48]:

255 $\eta_{ex=}\dfrac{W_{exp}+E_{evap}}{E_{in}}$ (22)

256 Where $E_{evap}$ is the cooling exergy through the evaporator and can be defined as [49-51]:

257 $E_{evap=}\dfrac{(\dot{m}c_p)_{evap}\int_0^{t_{cycle}}(T_{chill,o}-T_{chill,i})dt}{t_{cycle}}\left[\dfrac{T^{amb}}{T^{evap}}-1\right]$ (23)

258 While, $E_{in}$ is the exergy input to the system and can be defined as [17, 48]:

259 $E_{in=}\dot{m}_h\left[\left(h_{h,in}-h_{h,o}\right)-T^{amb}(s_{h,in}-s_{h,o})\right]$ (24)

## 260   5.  Results and discussions

261 Table 2 (a) shows the main operating conditions used in this work, while Table 2 (b) and (c) show the

262 features of the main components characteristics (bed, condenser, and evaporator) used in this study.

263 Figure 5 shows the values of COP/COPe, SCP/SCPe and exergy efficiency for two-bed basic cooling

264 adsorption system (BCAS) and adsorption system for cooling and electricity (with two-bed configuration)

265 for Silica-gel, AQSOA-Z02, and Aluminium-Fumarate with a range of heat source temperature. For most

266 cases, COPe achieved by the adsorption system for cooling and electricity using Silica-gel, Aluminium-

267 Fumarate, and AQSOA-Z02 is higher than the COP of BCAS and this is because additional electricity is

268 generated in adsorption system for cooling and electricity. However, for AQSOA-Z02 with heat source

269 temperature of 120 °C (or less), the COP of  BCAS is higher than COPe of adsorption system for cooling

270 and electricity and this is due to AQSOA- Z02 shows low performance with adsorption system for

271 cooling and electricity at low heat source temperatures. Moreover, SCPe achieved by the adsorption

272 system for cooling and electricity is higher than that produced by BCAS for most cases using Silica-gel,

273 Aluminium-Fumarate, and AQSOA-Z02 (except for Silica-gel at 80 °C and AQSOA-Z02 at 120 °C or

274 less and this is because less power is generated with low heat source temperatures). At high heat source

275 temperatures the mass flow rate of refrigerant (water) is higher because of high adsorption/desorption

13

rate. In addition, at high heat source temperatures, high pressure ratio can be obtained through the expander (turbine) which means more electricity can be generated. As the grade of electricity is higher than cooling (i.e. each 1kW of electricity produces about 3 kW of cooling depending on the typical COP for compression refrigeration system, which is assumed to be three in this study), SCPe of adsorption system for cooling and electricity is higher than that of BCAS at heat source temperature higher than 120 °C. For all adsorption materials and heat source temperatures used, the exergy efficiency achieved by adsorption system for cooling and electricity is higher than that for BCAS and this is because the electric power generated by the former has high grade than cooling. The maximum exergy efficiency of 54% is achieved using Silica-gel at heat source temperature of 80 °C, results also show that using adsorption system for cooling and electricity can enhance the exergy efficiency of BCAS by up to 2.5 times when using Al-Fumarate at heat source temperature of 160 °C. Also, results showed that, different adsorption materials presented different values of COP/COPe, SCP/SCPe, and exergy efficiency. For example, Silica-gel showed the highest COP and exergy efficiency, while AQSOA-Z02 showed the highest SCP with heat source temperature of 140 °C or higher. COP is the most important coefficient of any heat pump, because high COP values means less energy used. However, if the energy used is infinite or semi-infinite source like solar energy or geothermal energy, SCP can be the most important criterion, because high SCP means more cooling is generated using the same heat pump size. For system generating cooling and electricity, exergy efficiency is essential because the electricity has different grade compared to cooling, so it helps to make a good comparison between BCAS system and the adsorption system for cooling and electricity.

Figure 6, Figure 7, and Figure 8 show the cooling and power (electricity) generated using 7 different configurations utilizing Silica-gel, AQSOA-Z02 and Aluminium-Fumarate with heat source temperature of 120℃. Results show that cooling and electricity can be generated at the same time however, the amount of cooling and electricity generated is varied from one configuration to another and from one material to another. As the number of beds increases the amount of cooling and electricity increases because of more adsorption materials are added to the system and more uptake and mass flow can be generated. In addition, as the number of beds increases, more continuity in cooling and electricity can be noticed i.e. the cooling and electricity with less fluctuation which is more preferable. A significant gain in cooling and electricity can be noticed between 2B (two-beds) and 3B (three-bed) configurations where

14

305    more cooling and electricity can be generated with configuration 3B. Configuration 6B (six-beds) in

306    parallel with R=1/2 gives the highest average cooling and electricity generated as shown Figure 6, Figure

307    7, and Figure 8 for Silica-gel, AQSOA-Z02, and Aluminium-Fumarate respectively.

308    Figure 9 shows the COP of different configurations and R ratios utilizing Silica-gel, AQSOA-Z02, and

309    Aluminium-Fumarate with a range of heat source temperature between 80 and 160 °C. The maximum

310    COP achieved in this investigation is 0.64 using Silica-gel at heat source temperature of 80 °C with 2B

311    configuration and R=1. Compared to other materials at heat source temperature between 80-120 °C,

312    Silica-gel shows the highest COP and this is due to the high cooling capacity achieved with this material

313    as a result of high water uptake (high adsorption/desorption rate). Silica-gel's isotherms which has linear

314    and uniform shape, besides its good kinetics helps to generate such high uptake rate and this can explain

315    the high water and the high cooling capacity produced by this material. Regarding the heat source

316    temperature, at 80 °C the amount of heat consumed is the lowest which leads to highest COP. In terms of

317    the number of beds and R ratio used, the configuration 2B with R=1 shows the maximum COP and this is

318    due to less amount of heat when using 2B configuration.

319    Figure 10 shows SCP of different configurations and R ratios utilizing Silica-gel, AQSOA-Z02and

320    Aluminium-Fumarate with heat source temperature between 80 and 160 °C. The maximum SCP achieved

321    is around 650 W/kg$_{ads}$ Using AQSOA-Z02 at heat source temperature of 160 °C with three-bed

322    configuration and R=1/2. Generally, desorption rate is faster than adsorption rate [32] and this is because

323    the later occurs at relatively low temperature (28 °C in this study as an example), so discharging the

324    refrigerant (water) from the adsorption material can be faster than charging the materials with the

325    refrigerant. As a result, there is an optimum R ratio for each case depending on the adsorption material

326    and the regeneration temperature used. Again, this can explain why the configurations with R>1 have low

327    SCP compared to other configurations, as the time of adsorption is more than that of desorption.

328    Figure 11 shows SP of different configurations and R ratios utilizing Silica-gel, AQSOA-Z02 and

329    Aluminium-Fumarate with heat source temperature between 80 and 160 °C. Maximum SP generated in

330    this study is about 64 W/kg utilizing AQSOA-Z02 at 160 °C with 3B configuration and R=1/2. SP of 64

331    W/kg$_{ads}$ is not very large value compared to the value of cooling (650 W/kg$_{ads}$), however the grade of

332    electricity is higher than that of cooling because ideally each 1kW of electricity can generate 3kW of

333    cooling when the typical COP for compression refrigeration system is assumed to be 3. In terms of the

334  number of beds and R ratio used, the configuration 3B with R=½ has the maximum SP for Silica-gel and

335  Aluminium-Fumarate for all the range of heat source temperatures used, while for AQSOA-Z02 this

336  occurs only with heat source temperature of 160 °C and this can show that there is a specific limit of heat

337  source temperature, where after such limit the 3B configuration can be the best. The configurations with

338  R>1 have low SP compared to other configurations, as the time of adsorption is more than that of

339  desorption.

340  Figure 12 shows adsorption power efficiency of different configurations and R ratios utilizing Silica-gel,

341  AQSOA-Z02, and Aluminium-Fumarate with heat source temperature between 80 and 160 °C. The

342  maximum power efficiency achieved in this study is 4.63 % using AQSOA-Z02 at heat source

343  temperature of 160 °C with 2B configuration and R=1. As the heat source temperature increases, the mass

344  flow rate through the expander (turbine) increases because of high desorption rate. Moreover, high heat

345  source temperature produces more power and then high adsorption power efficiency and this is mainly

346  because the high pressure difference between the desorber and the condenser.

347  The main advantage of using multi-bed adsorption system for cooling and electricity is to increase the

348  values of SCP and SP generated from this system and offer better options to users and designers. Besides

349  increasing the quantity of the cooling and electricity, they can be generated with less fluctuation and more

350  continuity. However, using multi-bed adsorption configurations may lead to large size and heavy weight,

351  but this problem can be solved by developing new adsorption materials with better adsorption capacity,

352  and improving the design of the bed heat exchanger, besides using lighter and more efficient materials

353  in the bed heat exchanger. Also, this study shows that four-bed configuration consisting of a pair of two-

354  beds working in parallel produces more COP and SCP than the configuration with a same number of beds

355  working in series. The same result can be noticed for the six-bed configuration working in parallel

356  compared to the same number of beds working in series and this is due to R ratio used in each

357  configuration of R=1/2 and R=1/3 which produce the highest COP and SCP respectively.

358 **Table 2:**
359 **a)    Parameters used in simulation**

| Parameter | Value |
|---|---|
| Ambient temperature          $^{o}$C | 36 |
| Bed heating fluid temperature $^{o}$C | 80-140 |
| Bed cooling fluid temperature $^{o}$C | 28 |
| Condenser cooling temperature $^{o}$C | 28 |
| Chilled water temperature $^{o}$C | 18 |
| Bed hot fluid mass flow rate kg/s | 1.7 |
| Bed cold fluid mass flow rate kg/s | 1.6 |
| Condenser mass flow rate kg/s | 0.3 |
| Evaporator mass flow rate kg/s | 0.8 |
| Adsorption /desorption phase times (2 bed) | 300+20 |
| Switching time s | 20 |

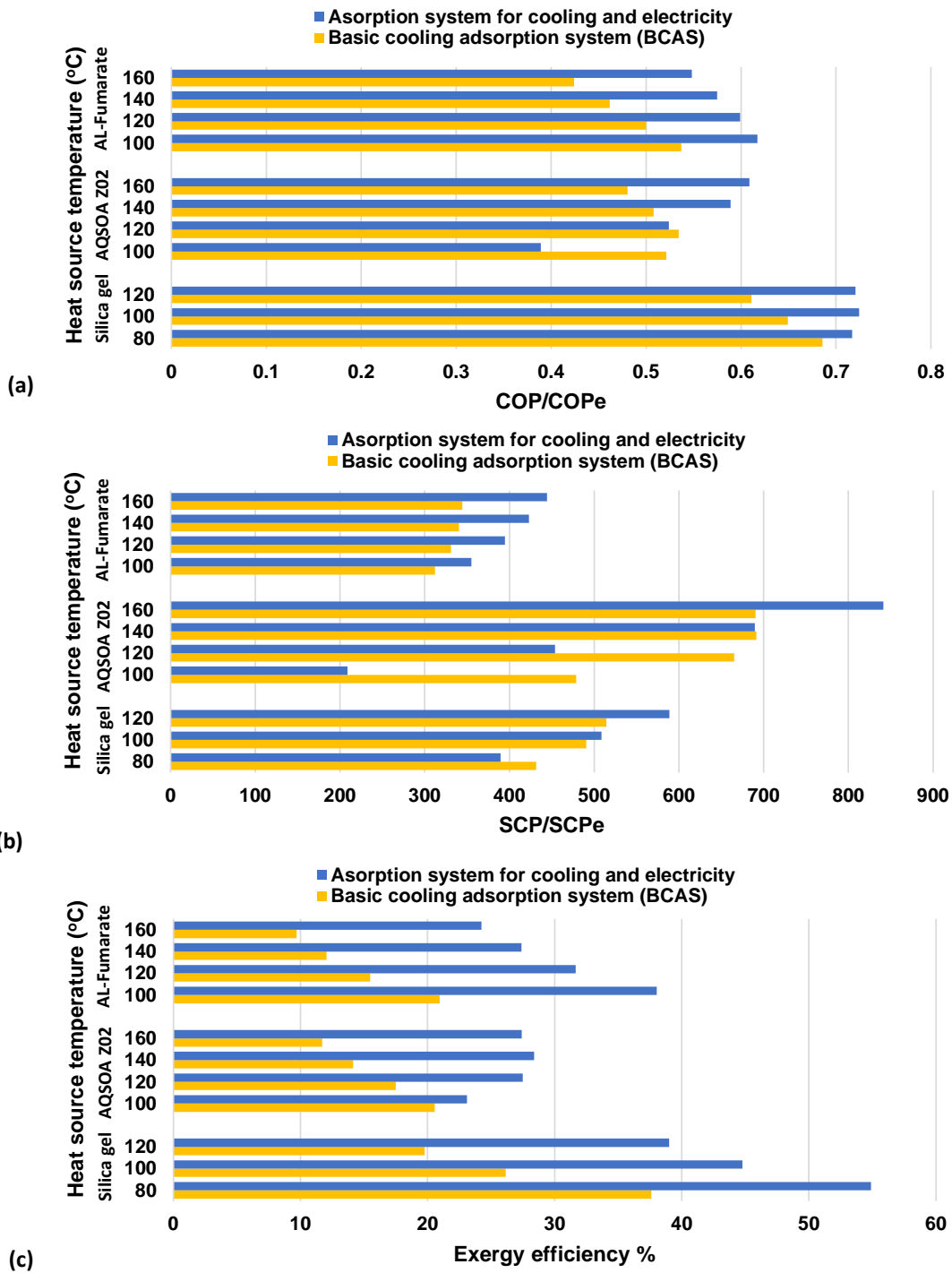366 **b)    Bed heat exchanger characteristics [26]**

| Parameter | Value |
|---|---|
| Fin length m | 172E-3 |
| Fin width  m | 30E-3 |
| Fin pitch m | 1.2E-3 |
| Module length m | 450E-3 |
| Finned length m | 370E-3 |
| No. of module | 4 |
| No. tubes/module | 6 |
| Tube OD  m | 15.875E-3 |
| Tube thickness m | 0.8E-3 |

367 **c)    Condenser/evaporator characteristics [26]**

| Parameter | Value |
|---|---|
| Pipe length m | 5.5 |
| No. tubes | 4 |
| Tube OD  m | 15.875E-3 |
| Tube thickness m | 0.8E-3 |

368

Figure 5: COP/COPe, SCP/SCPe and Exergy efficiency of basic cooling adsorption system (BCAS) and adsorption system for cooling and electricity (with two bed) for a range of heat source temperature utilizing Silica-gel, AQSOA-Z02 and Aluminium-Fumarate.
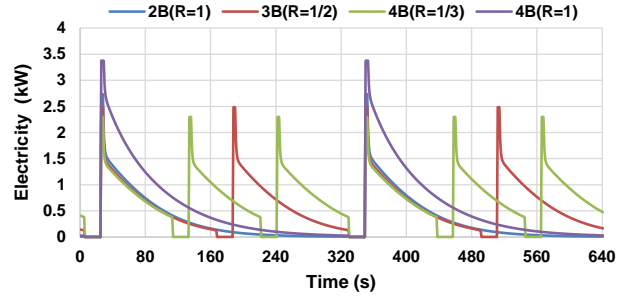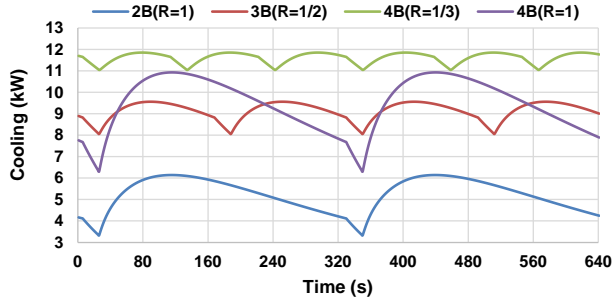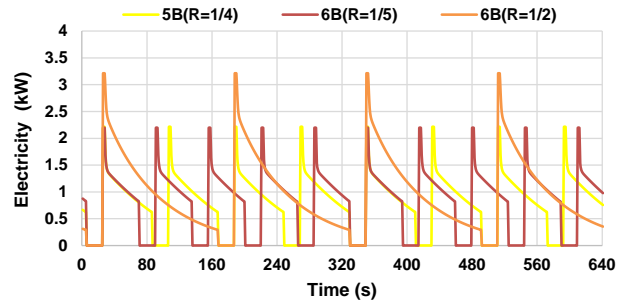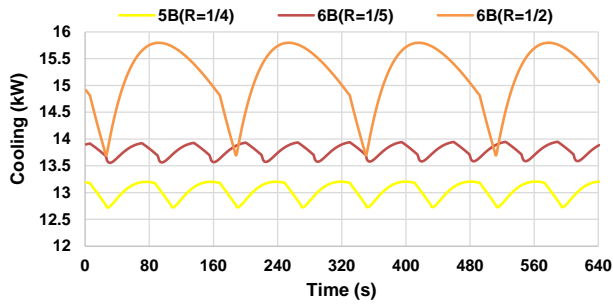
**Figure 6: Cooling and electricity generated from multi-bed adsorption system utilizing Silica-gel at heat source temperature of 120 °C.**
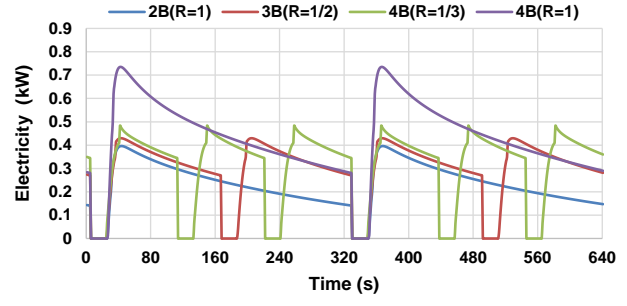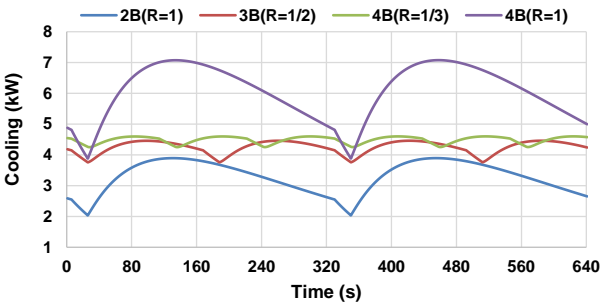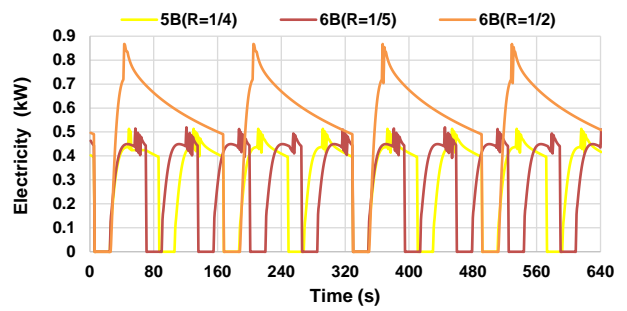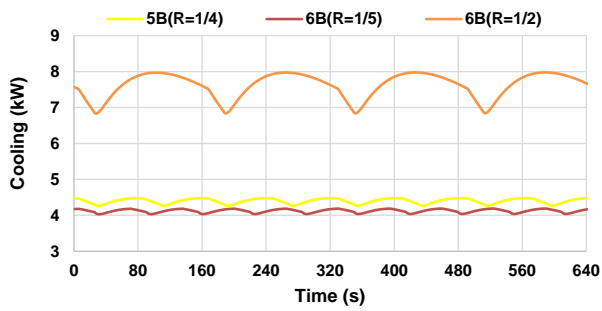


**Figure 7: Cooling and electricity generated from multi-bed adsorption system utilizing AQSOA-Z02 at heat source temperature of 120 °C.**
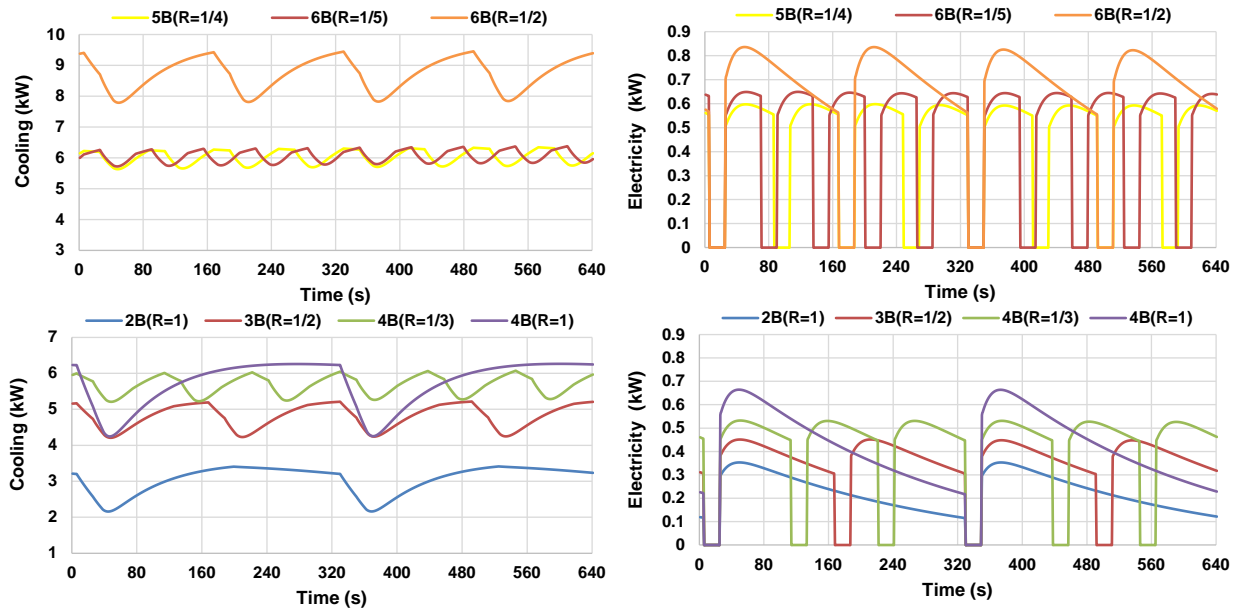
**Figure 8: Cooling and electricity generated from multi-bed adsorption system utilizing Aluminium-Fumarate at heat source temperature of 120 °C.**
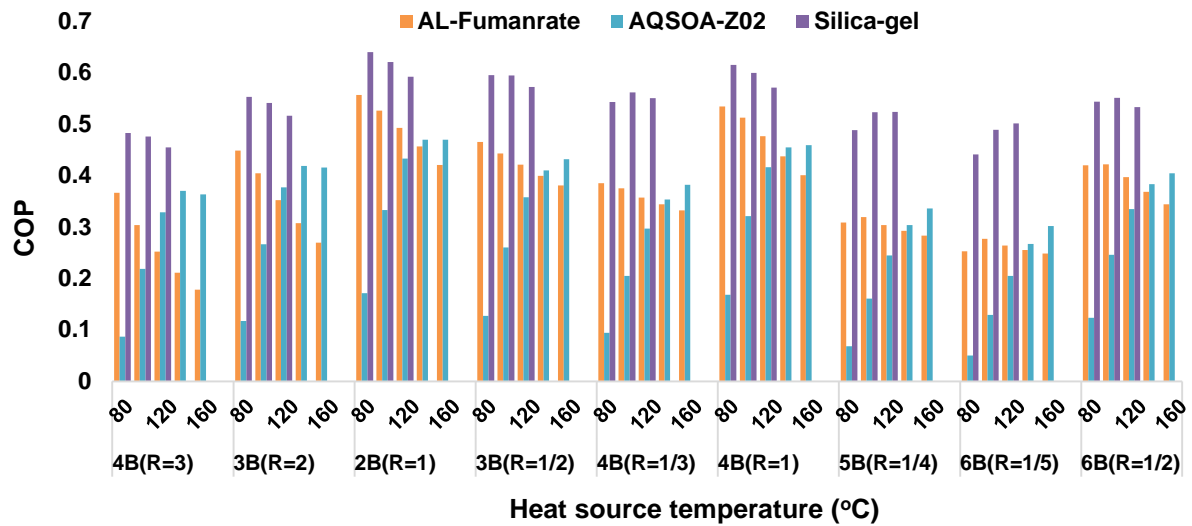


**Figure 9: COP of different configurations of multi-bed adsorption system and adsorption/desorption ratio (R) utilizing Silica-gel, AQSOA-Z02 and Aluminium-Fumarate with a range of heat source temperature.**
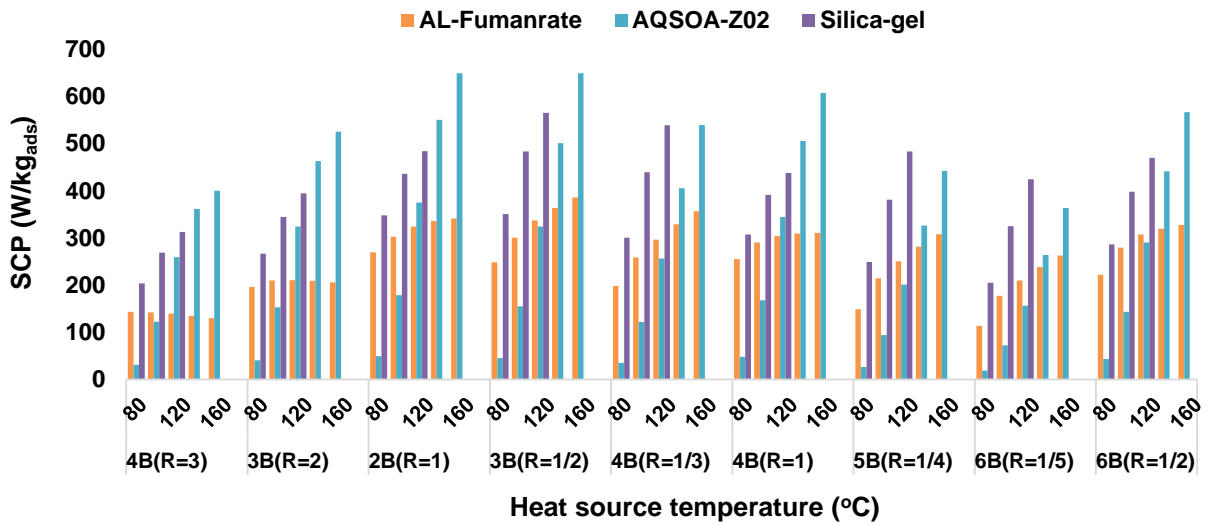
Figure 10: SCP of different configurations of multi-bed adsorption system and adsorption/desorption ratio (R) utilizing Silica-gel, AQSOA-Z02 and Aluminium-Fumarate with a range of heat source temperature.



Figure 11: SP of different configurations of multi-bed adsorption system and adsorption/desorption ratio (R) utilizing Silica-gel, AQSOA-Z02 and Aluminium-Fumarate with a range of heat source temperature.

**Figure 12: Adsorption power efficiency of different configurations of multi-bed adsorption system and adsorption/desorption ratio (R) utilizing Silica-gel, AQSOA-Z02 and Aluminium-Fumarate with a range of heat source temperature.**
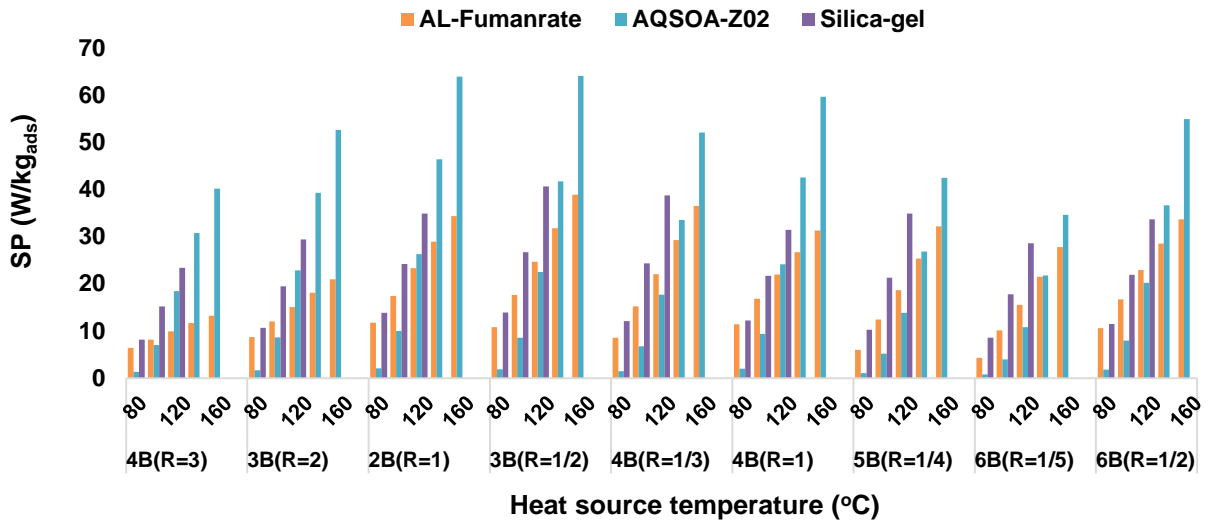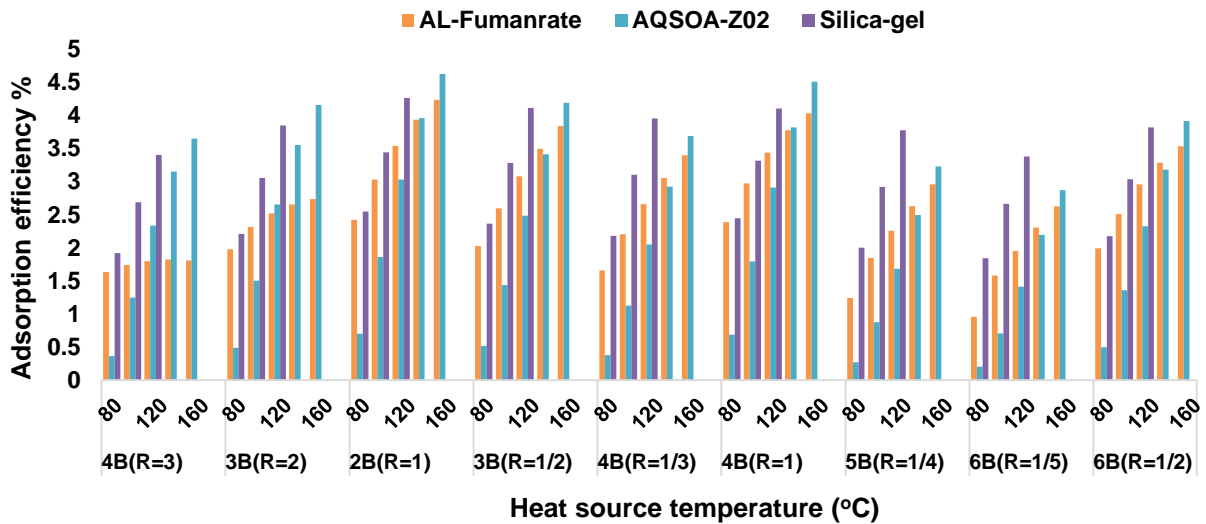
## 6. Conclusions

In this paper, 9 cases including 7 multi-bed adsorption system configurations and 7 different adsorption/desorption time ratios for generating cooling and electricity at the same time have been designed and simulated. Furthermore, advanced adsorption materials of AQSOA-Z02/water, Aluminium-Fumarate MOF/water, and Silica-gel/water are studied in terms of system performance and compared to each other. The main results of this study can be listed as:

1. Adsorption system for cooling and electricity is feasible and can generate cooling and electricity simultaneously. For example, utilizing 10.76 kg of Silica-gel at 120 °C of heat source temperature can generate an average cooling of 15.18 kW and an average electricity of 0.94 kW.

2. Adsorption system for cooling and electricity has higher COPe than basic cooling adsorption system (BCAS) except for AQSOA-Z02 with heat source temperature below 120 °C.

3. For all adsorption material and heat source temperatures used in this study, the exergy efficiency of adsorption system for cooling and electricity is higher than that for BCAS, and maximum exergy efficiency of 54% is achieved utilising Silica-gel at 80 °C.

4. Adsorption system for cooling and electricity has higher SCPe than BCAS for Silica-gel with heat source temperature higher than 100 °C, for AQSOA-Z02 with heat source temperature higher than 140 °C and for Aluminium-Fumarate with all heat source temperature used in this study.

5. Two-bed configuration with R=1 (adsorption/desorption time ratio =1) has the maximum COP for all adsorption materials and all range of temperatures used in this work.

22

421 6. Three-bed configuration with R=½ has the maximum SCP and SP for Silica-gel and Aluminium-

422 Fumarate for all the range of heat source temperatures used, while for AQSOA-Z02 with heat

423 source temperature of 160 °C.

424 7. As the number of beds increases more than two, the COP decreases, while as the number of beds

425 increases more than two or three (depending on martials and heat source temperature used) the SCP

426 and SP decrease.

427 8. As the number of bed increases, more continuity in cooling and electricity can be achieved.

428 9. Pairs of two-bed (four beds) and pairs of three-bed (six beds) configurations working in parallel

429 produce more COP and SCP than four-bed and six-bed configurations working in series.

430 **Nomenclature**

| *Symbols* | | | |
|---|---|---|---|
| $A$ | adsorption potential, J/mole | $\eta$ | efficiency |
| $Al$ | aluminium | $\alpha$ | constant used in eq. 2 |
| $A_r$ | area, $m^2$ | $\rho$ | density $kg/m^3$ |
| $C_p$ | specific heat capacity, J/kg.K | $\varphi$ | flag |
| COP | coefficient of performance | *Subscript* | |
| COPe | equivalent coefficient of performance | ads,a | adsorbent |
| $E$ | Exergy  kW | ads | adsorption |
| $k_o$ | empirical constant in Eq. (6), 1/s | amb | ambient temperature |
| $E_a$ | activation energy, J/kg | bed | adsorbent bed |
| $h$ | enthalpy,  J/kg | chill | chilled water |
| $h_{fg}$ | evaporation latent heat J/kg | cond | condenser |
| $M$ | mass, kg | des | desorption |
| $\dot{m}$ | mass flow rate, kg/s | eff | effective |
| $P$ | pressure, Pa | evap,e | evaporator |
| $Q_{st}$ | isosteric heat of adsorption, J/kg | exp | expander |
| $R$ | gas constant (for water vapour), J/kg.K | ex | exergy |
| $R$ | adsorption/desorption time ratio | f | liquid |
| $U$ | overall heat transfer coff., $W/m^2K$ | g | gas |
| $W$ | power generated W | i | adsorption/desorption |
| SP | specific power generated $W/kg_{ads}$ | in | inlet |
| SCP | specific cooling power $W/kg_{ads}$ | j | cooling / heating  source |
| SCPe | equivalent specific cooling power $W/kg_{ads}$ | h | hot,heating source |
| $t$ | time, s | n | constant used in eq. 2 |
| $T$ | temperature, K | o | outlet |
| $x$ | adsorption uptake, $kg/kg_{ads}$ | s | saturation |
| $x_{eq}$ | equilibrium uptake, $kg/kg_{ads}$ | w | water |

431

432

433

434

435

## REFRENCES

1.  Cai, D., et al., *Experimental evaluation on thermal performance of an air-cooled absorption refrigeration cycle with NH3–LiNO3 and NH3–NaSCN refrigerant solutions.* Energy Conversion and Management, 2016. **120**: p. 32-43.

2.  Gomri, R., *Simulation study on the performance of solar/natural gas absorption cooling chillers.* Energy Conversion and Management, 2013. **65**: p. 675-681.

3.  Jribi, S., et al., *Modeling and simulation of an activated carbon–CO2 four bed based adsorption cooling system.* Energy Conversion and Management, 2014. **78**: p. 985-991.

4.  Ali, S.M. and A. Chakraborty, *Adsorption assisted double stage cooling and desalination employing silica gel+water and AQSOA-Z02+water systems.* Energy Conversion and Management, 2016. **117**: p. 193-205.

5.  Askalany, A.A., et al., *An overview on adsorption pairs for cooling.* Renewable and Sustainable Energy Reviews, 2013. **19**: p. 565-572.

6.  Mitra, S., et al., *Modeling study of two-stage, multi-bed air cooled silica gel+water adsorption cooling cum desalination system.* Applied Thermal Engineering, 2017. **114**: p. 704-712.

7.  Zhao, H., et al., *Mechanical and experimental study on freeze proof solar powered adsorption cooling tube using active carbon/methanol working pair.* Energy Conversion and Management, 2008. **49**(8): p. 2434-2438.

8.  González-Gil, A., et al., *Experimental evaluation of a direct air-cooled lithium bromide–water absorption prototype for solar air conditioning.* Applied Thermal Engineering, 2011. **31**(16): p. 3358-3368.

9.  Wang, R.Z., *Efficient adsorption refrigerators integrated with heat pipes.* Applied Thermal Engineering, 2008. **28**(4): p. 317-326.

10. Gong, L.X., et al., *Experimental study on an adsorption chiller employing lithium chloride in silica gel and methanol.* International Journal of Refrigeration, 2012. **35**(7): p. 1950-1957.

11. Modi, A., et al., *Thermoeconomic optimization of a Kalina cycle for a central receiver concentrating solar power plant.* Energy Conversion and Management, 2016. **115**: p. 276-287.

12. Chen, T., et al., *A novel cascade organic Rankine cycle (ORC) system for waste heat recovery of truck diesel engines.* Energy Conversion and Management, 2017. **138**: p. 210-223.

13. Le, V.L., et al., *Performance optimization of low-temperature power generation by supercritical ORCs (organic Rankine cycles) using low GWP (global warming potential) working fluids.* Energy, 2014. **67**: p. 513-526.

14. Vijayaraghavan, S. and D.Y. Goswami, *A combined power and cooling cycle modified to improve resource utilization efficiency using a distillation stage.* Energy, 2006. **31**(8-9): p. 1177-1196.

15. Liu, M. and N. Zhang, *Proposal and analysis of a novel ammonia–water cycle for power and refrigeration cogeneration.* Energy, 2007. **32**(6): p. 961-970.

16. Zheng, D., et al., *Thermodynamic analysis of a novel absorption power/cooling combined-cycle.* Applied Energy, 2006. **83**(4): p. 311-323.

17. Zhang, N. and N. Lior, *Development of a Novel Combined Absorption Cycle for Power Generation and Refrigeration.* Journal of Energy Resources Technology, 2007. **129**(3): p. 254.

18. Bargman, R., *Adsorption vs. Absorption Chillers: Applications and Use Overview.* Hub Pages, 2010.

19. H.T. Chua, K.C.N., A. Malek, T. Kashiwagi, A. Akisawa, B.B. Saha *Multi-bed regenerative adsorption chiller-improving the utilization of waste heat and reducing the chilled water outlet temperature fluctuation.* International Journal of Refrigeration, 2001. **24**: p. 124-136.

485   20.   Jiang, L., et al., *Design and performance analysis of a resorption cogeneration system.*
486         International Journal of Low-Carbon Technologies, 2013. **8**(suppl 1): p. i85-i91.
487   21.   Wang, L., et al., *A resorption cycle for the cogeneration of electricity and refrigeration.* Applied
488         Energy, 2013. **106**: p. 56-64.
489   22.   Bao, H., Y. Wang, and A.P. Roskilly, *Modelling of a chemisorption refrigeration and power*
490         *cogeneration system.* Applied Energy, 2014. **119**: p. 351-362.
491   23.   Bao, H., et al., *Chemisorption cooling and electric power cogeneration system driven by low*
492         *grade heat.* Energy, 2014. **72**: p. 590-598.
493   24.   Jiang, L., et al., *Performance prediction on a resorption cogeneration cycle for power and*
494         *refrigeration with energy storage.* Renewable Energy, 2015. **83**: p. 1250-1259.
495   25.   Lu, Y., et al., *Analysis of an optimal resorption cogeneration using mass and heat recovery*
496         *processes.* Applied Energy, 2015. **160**: p. 892-901.
497   26.   Al-Mousawi, F.N., R. Al-Dadah, and S. Mahmoud, *Low grade heat driven adsorption system for*
498         *cooling and power generation using advanced adsorbent materials.* Energy Conversion and
499         Management, 2016. **126**: p. 373-384.
500   27.   Al-Mousawi, F.N., R. Al-Dadah, and S. Mahmoud, *Low grade heat driven adsorption system for*
501         *cooling and power generation with small-scale radial inflow turbine.* Applied Energy, 2016. **183**:
502         p. 1302-1316.
503   28.   Al-Mousawi, F.N., R. Al-Dadah, and S. Mahmoud, *Integrated adsorption-ORC system:*
504         *Comparative study of four scenarios to generate cooling and power simultaneously.* Applied
505         Thermal Engineering, 2017. **114**: p. 1038-1052.
506   29.   Alam, K.C.A., et al., *A novel approach to determine optimum switching frequency of a*
507         *conventional adsorption chiller.* Energy, 2003. **28**(10): p. 1021-1037.
508   30.   Sapienza, A., et al., *Influence of the management strategy and operating conditions on the*
509         *performance of an adsorption chiller.* Energy, 2011. **36**(9): p. 5532-5538.
510   31.   Saha, B.B., et al., *Performance evaluation of a low-temperature waste heat driven multi-bed*
511         *adsorption chiller.* International Journal of Multiphase Flow, 2003. **29**(8): p. 1249-1263.
512   32.   Glaznev, I.S. and Y.I. Aristov, *The effect of cycle boundary conditions and adsorbent grain size on*
513         *the water sorption dynamics in adsorption chillers.* International Journal of Heat and Mass
514         Transfer, 2010. **53**(9-10): p. 1893-1898.
515   33.   Sapienza, A., et al., *Adsorption chilling driven by low temperature heat: New adsorbent and cycle*
516         *optimization.* Applied Thermal Engineering, 2012. **32**: p. 141-146.
517   34.   Zajaczkowski B. Performance analysis and cycle time optimization of a single evaporator three-
518         bed solid-sorption refrigeration system driven by lowtemperature heat source, ICR 2015,
519         Conference Proceedings Yokohama, Japan; 2015
520   35.   Graf, S., et al., *Prediction of SCP and COP for adsorption heat pumps and chillers by combining*
521         *the large-temperature-jump method and dynamic modeling.* Applied Thermal Engineering, 2016.
522         **98**: p. 900-909.
523   36.   Al-Mousawi, F.N., Raya Al-Dadah, and Saad Mahmoud, *Novel adsorption system for cooling and*
524         *power generation utilizing low grade heat sources.* Students on Applied Engineering (ISCAE),
525         International Conference for. IEEE, 2016.
526   37.   Sun, B. and A. Chakraborty, *Thermodynamic formalism of water uptakes on solid porous*
527         *adsorbents for adsorption cooling applications.* Applied Physics Letters, 2014. **104**(20): p.
528         201901.
529   38.   Elsayed, E., et al., *Aluminium fumarate and CPO-27(Ni) MOFs: Characterization and*
530         *thermodynamic analysis for adsorption heat pump applications.* Applied Thermal Engineering,
531         2016. **99**: p. 802-812.
532   39.   Miyazaki, T., et al., *A new cycle time allocation for enhancing the performance of two-bed*
533         *adsorption chillers.* International Journal of Refrigeration, 2009. **32**(5): p. 846-853.
534   40.   Saha, B.B., et al., *Waste heat driven dual-mode, multi-stage, multi-bed regenerative adsorption*
535         *system.* International Journal of Refrigeration, 2003. **26**(7): p. 749-757.

536 41. El-Sharkawy, I.I., H. AbdelMeguid, and B.B. Saha, *Towards an optimal performance of adsorption*
537 *chillers: Reallocation of adsorption/desorption cycle times.* International Journal of Heat and
538 Mass Transfer, 2013. **63**: p. 171-182.
539 42. Hassan, H.Z., et al., *A review on the equations of state for the working pairs used in adsorption*
540 *cooling systems.* Renewable and Sustainable Energy Reviews, 2015. **45**: p. 600-609.
541 43. Sadeghlu, A., et al., *Performance evaluation of Zeolite 13X/CaCl2 two-bed adsorption*
542 *refrigeration system.* International Journal of Thermal Sciences, 2014. **80**: p. 76-82.
543 44. Youssef, P.G., S.M. Mahmoud, and R.K. Al-Dadah, *Performance analysis of four bed adsorption*
544 *water desalination/refrigeration system, comparison of AQSOA-Z02 to silica-gel.* Desalination,
545 2015. **375**: p. 100-107.
546 45. Saha, B.B., Elisa C. Boelman, and Takao Kashiwagi, *Computational analysis of an advanced*
547 *adsorption-refrigeration cycle.* Energy, 1995. **20**(10): p. 983-994.
548 46. Tso, C.Y., C.Y.H. Chao, and S.C. Fu, *Performance analysis of a waste heat driven activated carbon*
549 *based composite adsorbent – Water adsorption chiller using simulation model.* International
550 Journal of Heat and Mass Transfer, 2012. **55**(25-26): p. 7596-7610.
551 47. Farid, S.K., et al., *A numerical analysis of cooling water temperature of two-stage adsorption*
552 *chiller along with different mass ratios.* International Communications in Heat and Mass
553 Transfer, 2011. **38**(8): p. 1086-1092.
554 48. Wang, J., et al., *Thermodynamic analysis of a new combined cooling and power system using*
555 *ammonia–water mixture.* Energy Conversion and Management, 2016. **117**: p. 335-342.
556 49. Koronaki, I.P., E.G. Papoutsis, and V.D. Papaefthimiou, *Thermodynamic modeling and exergy*
557 *analysis of a solar adsorption cooling system with cooling tower in Mediterranean conditions.*
558 Applied Thermal Engineering, 2016. **99**: p. 1027-1038.
559 50. Zhai, H., et al., *Energy and exergy analyses on a novel hybrid solar heating, cooling and power*
560 *generation system for remote areas.* Applied Energy, 2009. **86**(9): p. 1395-1404.
561 51. Bellos, E., C. Tzivanidis, and K.A. Antonopoulos, *Exergetic, energetic and financial evaluation of a*
562 *solar driven absorption cooling system with various collector types.* Applied Thermal
563 Engineering, 2016. **102**: p. 749-759.
564